Synthesis and Structure Determination of the Linear Conjugated Polyynyl and Polyynediyl Iron Complexes Fp*−(C≡C)$_n$−X (X = H (n = 1, 2); X = Fp* (n = 1, 2, 4); Fp* = (η^5-C$_5$Me$_5$)Fe(CO)$_2$)[1]

Munetaka Akita,* Min-Chul Chung, Aizoh Sakurai, Shuichiro Sugimoto, Masako Terada, Masako Tanaka, and Yoshihiko Moro-oka*

Research Laboratory of Resources Utilization, Tokyo Institute of Technology, 4259 Nagatsuta, Midori-ku, Yokohama 226, Japan

Received June 26, 1997[⊗]

A series of polyynyl and polyynediyl complexes of iron, Fp*−(C≡C)$_n$−H [n = 2 (**3**)) and Fp*−(C≡C)$_n$−Fp* (n = 2 (**4**), 4 (**5**); Fp* = (η^5-C$_5$Me$_5$)Fe(CO)$_2$), have been prepared, and their linear structure has been confirmed by X-ray crystallography.

Introduction

The chemistry of polyynediyl−dimetal complexes, M−(C≡C)$_n$-M, has attracted increasing attention from various viewpoints.[2] The pioneering work done by Prof. Hagihara's group[3] has been followed by many research groups, and the length of the carbon chain reached C$_{20}$, as recently reported by Gladysz et al.[4h] The π-conjugated polycarbon system is extended to the two terminal metal units, and such systems are expected to display attractive properties resulting from (i) π-conjugation along the rodlike linkage, (ii) stabilization of odd-electron (mixed-valent) species formed by oxidation and reduction, and (iii) hyperpolarizability. In addition to this feature, polycarbon species (C$_n$) coordinated with metal systems, in particular, incorporated in a polymetallic environment, can be viewed as structural models of carbide species adsorbed on a heterogeneous catalyst surface. In our laboratory, synthetic work has been directed toward the latter subject.[5] As a result, a variety of polynuclear C$_2$ and C$_2$H complexes have been prepared by addition of metal fragments to the parent acetylide complexes, i.e. ethynyl (Fp*−C≡CH; **1** (C$_2$H)) and ethynediyl complexes (Fp*−C≡C−Fp*; **2** (μ-C$_2$)). Now we are extending synthetic efforts to polycarbon complexes M$_m$(C$_n$) other than those with n = 2,[6] and herein we disclose the synthesis and structure determination of the butadiynyl (Fp*−C≡CC≡CH; **3** (C$_4$H)), butadiynediyl (Fp*−C≡CC≡C−Fp*; **4** (μ-C$_4$)), and octatetraynediyl complexes (Fp*−C≡CC≡CC≡CC≡C−Fp*; **5** (μ-C$_8$)). The structures of the related ethynyl (**1**) and ethynediyl complexes (**2**) are also discussed as comparative systems, although their synthesis and the structure determination of **1** were already reported in a previous paper.[5b]

Scheme 1

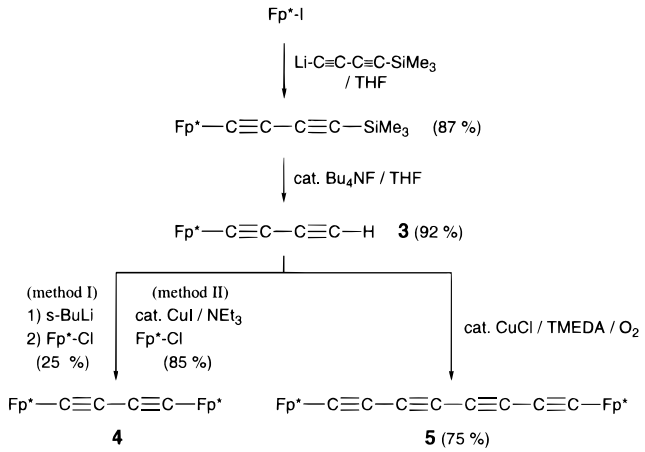

Results and Discussion

Synthesis of Butadiynyl (3), Butadiynediyl (4), and Octatetraynediyl Complexes (5). The butadiynyl complex Fp*−C≡CC≡CH (**3**) was prepared according to the synthetic procedure reported for the Fp

[⊗] Abstract published in *Advance ACS Abstracts,* October 15, 1997.

(1) Abbreviations used in this paper: Cp* = η^5-C$_5$Me$_5$; Cp$^\#$ = η^5-C$_5$Me$_4$Et; Cp = η^5-C$_5$H$_5$; Fp* = Cp*Fe(CO)$_2$; Fp$^\#$ = Cp$^\#$Fe(CO)$_2$; Fp = CpFe(CO)$_2$.

(2) (a) Beck, W.; Niemer, B.; Wieser, M. *Angew. Chem., Int. Ed. Engl.* **1993**, *32*, 923. (b) Lang, H. *Angew. Chem., Int. Ed. Engl.* **1994**, *33*, 547. (c) Bunz, U. *Angew. Chem., Int. Ed. Engl.* **1996**, *35*, 969.

(3) (a) Sonogashira, K.; Fujikura, Y.; Yatake, T.; Toyoshima, N.; Takahashi, S.; Hagihara, N. *J. Orgaonomet. Chem.* **1978**, *145*, 101. (b) Sonogashira, K.; Kataoka, S.; Takahashi, S.; Hagihara, N. *J. Orgaonomet. Chem.* **1978**, *160*, 319. (c) Sonogashira, K.; Ohga, K.; Takahashi, S.; Hagihara, N. *J. Orgaonomet. Chem.* **1980**, *188*, 237. (d) Ogawa, H.; Onitsuka, K.; Joh, T.; Takahashi, S. *Organometallics* **1988**, *7*, 2257.

(4) (a) Ramsden, J. A.; Arif, A.; Gladysz, J. A. *J. Am. Chem. Soc.* **1992**, *114*, 6809. (b) Ramsden, J. A.; Weng, W.; Gladysz, J. A. *Organometallics* **1992**, *11*, 3635. (c) Zhou, Y.; Seyler, J. W.; Weng, W.; Arif, A. M.; Gladysz, J. A. *J. Am. Chem. Soc.* **1993**, *115*, 8509. (d) Seyler, J. W.; Weng, W.; Zhou, Y.; Gladysz, J. A. *Organometallics* **1993**, *12*, 3802. (e) Weng, W.; Bartik, T.; Gladysz, J. A. *Angew. Chem., Int. Ed. Engl.* **1994**, *33*, 2199. (f) Brady, M.; Weng, W.; Gladysz, J. A. *J. Chem. Soc., Chem. Commun.* **1994**, 2655. (g) Weng, W.; Bartik, T.; Brady, M.; Bartik, B.; Ramsden, J. A.; Arif, A. M.; Gladysz, J. A. *J. Am. Chem. Soc.* **1995**, *117*, 11922. (h) Bartik, T.; Bartik, B.; Brady, M.; Dembinski, R.; Gladysz, J. A. *Angew. Chem., Int. Ed. Engl.* **1996**, *35*, 414. (i) Brady, M.; Weng, W.; Zhou, Y.; Seyler, J. W.; Amoroso, A. J.; Arif, A. M.; Böhme, M.; Frenking, G.; Gladysz, J. *J. Am. Chem. Soc.* **1997**, *119*, 775.

(5) (a) Akita, M.; Moro-oka, Y. *Bull. Chem. Soc. Jpn.* **1995**, *68*, 420. (b) Akita, M.; Terada, M.; Oyama, S.; Moro-oka, Y. *Organometallics* **1990**, *9*, 816. (c) Akita, M.; Terada, M.; Oyama, S.; Sugimoto, S.; Moro-oka, Y. *Organometallics* **1991**, *10*, 1561. (d) Akita, M.; Terada, M.; Moro-oka, Y. *Organometallics* **1991**, *10*, 2961. The reaction mechanism has been corrected in ref 5e. (e) Akita, M.; Takabuchi, A.; Terada, M.; Ishii, N.; Tanaka, M.; Moro-oka, Y. *Organometallics* **1994**, *13*, 2516. (f) Terada, M.; Masaki, Y.; Tanaka, M.; Akita, M.; Moro-oka, Y. *J. Chem. Soc., Chem. Commun.* **1995**, 1611. (g) Akita, M.; Kato, S.; Terada, M.; Masaki, Y.; Tanaka, M.; Moro-oka, Y. *Organometallics* **1997**, *16*, 2392.

(6) C$_1$ complex: Takahashi, Y.; Akita, M.; Moro-oka, Y. *J. Chem. Soc., Chem. Commun.* **1997**, 1557.

S0276-7333(97)00538-4 CCC: $14.00

Table 1. Spectroscopic Data for Fp*−(C≡C)$_n$−Fp* and Fp*−(C≡C)$_n$H Complexes[a]

complex (ligand)	^{13}C NMR[b,c]/ppm							IR/cm^{-1}			
	^{1}H NMR/ppm Cp* (s)	C_α	C_β	C_γ	C_δ	C_5Me_5	C_5Me_5[d]	CO	ν(C≡C)	ν(CO)	ν(≡CH)
3 (C_4H)	1.85[e]	106.4	92.8 (d, 7)	71.9 (d, 50)	53.5 (d, 252)	97.4	9.8	213.4	2141[f]	2022,1993 1966, 1935[f]	3307[f]
									2141[g]	2027,1977[g]	3303[g]
4 (μ-C_4)	1.83	79.8[h]	98.5[h]	98.5[h]	79.8[h]	96.9	10.0	214.5	2146 2150	2010, 1989, 1949[f] 2020, 1968[g]	
5 (μ-C_8)	1.83	110.8[h]	94.8[h]	61.6[h]	51.4[h]	98.2	9.9	213.8	2137, 2086 2136, 2088	2016, 1972[f] 2028, 1981[g]	
1[j,k] (C_2H)	1.44[l]	97.0 (d, 55)	97.5 (d, 227)			96.7	9.6	215.5	*i*	2005, 1966[f] 2022, 1968[g]	3281[f] 3278[g]
2[j,k] (μ-C_2)	1.78	98.1	98.1			96.2	9.9	217.5	*i*	1995, 1953[f] 1996, 1951[g]	

[a] NMR spectra (^{1}H NMR, 400 MHz; ^{13}C NMR, 100 MHz) were observed in $CDCl_3$ (**3**, **4**) and CD_2Cl_2 (**5**). [b] Fe−C_α−C_β−C_γ−C_δ. [c] Singlet signals unless otherwise stated. [d] Quartet signals with J_{C-H} = ∼125 Hz. [e] δ_H(C_4H) 1.42. [f] KBr pellets. [g] In CH_2Cl_2. [h] Tentatively assigned (see text). [i] Not observed. [j] Reference 5b. [k] NMR in C_6D_6. [l] δ_H(C_2H) 1.99.

derivative by Wong et al. (Scheme 1).[7b] The (trimethylsilyl)butadiynyl complex was prepared by metathesis between Fp*−I and ((trimethylsilyl)butadiynyl)lithium which was generated by treatment of bis(trimethylsilyl)-butadiyne with MeLi. Subsequent desilylation with a catalytic amount of Bu_4NF gave **3** as orange crystals. Conversion of Fp−C≡CC≡CH (the Fp derivative of **3**) into the butadiynediyl complex (Fp−C≡CC≡C−Fp) was also reported by Wong, but application of this procedure to the Fp* system (successive treatment with *s*-BuLi and Fp*−Cl; method I) afforded the desired product **4** in 25% yield. Instead, complex **4** was successfully prepared in a good yield (85%) by means of a Cu-catalyzed coupling reaction[8a] between **3** and Fp*−Cl (method II). The oxidative Cu-mediated reaction of **3** resulted in homodimerization of the Fp*−C_4 unit to give the octatetraynediyl complex **5** in 75% yield.[8] The synthesis of the tungsten analogue of **5** via a similar preparative method was already reported by Bruce et al.[9b]

The obtained polyynyl and polyynediyl complexes were readily characterized by spectroscopic analysis, in particular, by ^{13}C NMR and ν(C≡C) IR data (Table 1), and selected spectral and structural data for related C_n and C_nH complexes are summarized in Table 2.

The ^{13}C NMR data for the C_4H carbon atoms in butadiynyl complexes (M−C≡CC≡CH), including **3**, are unequivocally assigned on the basis of the J_{C-H} or J_{C-P} values. In general, the α-carbon atom is at the lowest field and the ^{13}C NMR signals of the C_4H moiety appear in the order $C_\alpha > C_\beta > C_\gamma > C_\delta$ (δ_C values).

On the other hand, assignment of the ^{13}C NMR data of butadiynediyl (M−C≡CC≡C−M) and octatetraynediyl complexes (M−C≡CC≡CC≡CC≡C−M) can be made only for complexes containing an NMR-active metal or auxiliary (X such as ^{183}W and ^{31}P) on the basis of the magnitude of the J_{C-X} coupling constants. The ^{13}C NMR signals of butadiynediyl complexes appear in the order (δ_C values: $C_{\beta,\gamma} > C_{\alpha,\delta}$) opposite to that of the butadiynyl complexes, as summarized in Table 2, and the data for **4** are tentatively assigned according to this tendency.

To our knowledge, only three examples of octatetraynediyl complexes bearing ReCp*(NO)(PPh_3),[4f] FeCp*-(dppe),[11 c] and $WCp(CO)_3$ fragments[9b] have been reported so far. The ^{13}C signals of the C_8 bridge shift downfield as the carbon atoms become closer to the metal center (δ_C values: $C_\alpha > C_\beta > C_\gamma > C_\delta$), with the exception of the Re compound, where the α-carbon signal was located at slightly higher field than was the β-carbon signal. The ^{13}C NMR data for the rhenium and iron complexes were assigned on the basis of the J_{P-C} couplings as well as by comparison with the data for the corresponding C_4H and μ-C_4 complexes, and the grounds of the assignment of the tungsten complex appear to be the broadening of the α-carbon signal due to the satellite peaks resulting from coupling with the ^{183}W nucleus. The signals of **5** are tentatively assigned as shown in Table 1 according to this tendency, and the chemical shift values are found to be very close to those of the previously reported iron and tungsten complexes.

The deshielding of the α-carbon signals of the butadiynyl (**3**) and octatetraynediyl complexes (**5**) is attributable to the contribution of the cumulenylidene-type structure resulting from back-donation from the metal center (Chart 1). Because the α-carbon atom of $HC_\alpha{\equiv}C_\beta OEt$, a 1-alkyne bearing a π-electron-donating substituent, appears at very high field (δ_C 23.2) compared with the terminal carbon signals of 1-alkynes (65−80 ppm),[16] the higher field shift of the C_δ signals of **3** and **5** suggests

(7) (a) Kim, P. J.; Masai, M.; Sonogashira, K.; Hagihara, N. *Inorg. Nucl. Chem. Lett.* **1970**, *6*, 181. (b) Wong, A.; Kang, P. C. W.; Tagge, C. D.; Leon, D. R. *Organometallics* **1990**, *9*, 1992. (c) Crescenzi, R.; Lo Sterzo, C. *Organometallics* **1992**, *11*, 4301.

(8) (a) Taylor, R. J. *Practical Approach Series in Organic Synthesis: Organocopper Reagents*; Oxford University Press: Oxford, U.K., 1995; see also references cited therein. (b) The procedure for the synthesis of **5** followed that for oxidative dimerization of (trimethylsilyl)acetylene leading to 1,4-bis(trimethylsilyl)butadiyne.[25a] (c) See also: Bruce, M. I.; Humphrey, M. G.; Matisons, J. G.; Roy, S. C.; Swincer, A. G. *Aust. J. Chem.* **1984**, *37*, 1955.

(9) (a) Bruce, M. I.; Hinterding, P.; Tiekink, E. R. T.; Skelton, B. W.; White, A. H. *J. Organomet. Chem.* **1993**, *450*, 209. (b) Bruce, M. I.; Ke, M.; Low, P. J. *J. Chem. Soc., Chem. Commun.* **1996**, 2405. (c) Bruce, M. I.; Skelton, B. W.; White, A. H.; Zaitseva, N. N. *J. Chem. Soc., Dalton Trans.* **1996**, 3151.

(10) Davison, A.; Selegue, J. P. *J. Am. Chem. Soc.* **1978**, *100*, 7763.

(11) (a) Le Narvoir, N.; Lapinte, C. *J. Chem. Soc., Chem. Commun.* **1993**, 357. (b) Le Narvoir, N.; Toupet, L.; Lapinte, C. *J. Am. Chem. Soc.* **1995**, *117*, 7129. (c) Coat, F.; Lapinte, C. *Organometallics* **1996**, *15*, 477.

(12) (a) Kousantonis, G. A.; Selegue, J. P. *J. Am. Chem. Soc.* **1991**, *113*, 2316. (b) Lomprey, J. R.; Selegue, J. P. *J. Am. Chem. Soc.* **1992**, *114*, 5518.

(13) Touchard, D.; Haquette, P.; Pirio, N.; Toupet, L.; Dixneuf, P. H. *Organometallics* **1993**, *12*, 2062.

(14) (a) Sun, Y.; Taylor, N. J.; Carty, A. J. *J. Organomet. Chem.* **1992**, *423*, C43. (b) Sun, Y.; Taylor, N. J.; Carty, A. J. *Organometallics* **1992**, *11*, 4293.

(15) St. Clair, M.; Schaefer, W. P.; Bercaw, J. E. *Organometallics* **1991**, *10*, 525.

(16) (a) Clerc, P.; Simon, S. *Tables for Structure Determination of Organic Compounds by Spectroscopic Methods*; Springer: Berlin, 1981. (b) March, J. *Advanced Organic Chemistry*, 3rd ed.; Wiley: New York, 1985.

(17) (a) Appel, M.; Heidrich, J.; Beck, W. *Chem. Ber.* **1987**, *120*, 1087. (b) Heidrich, J.; Steimann, M.; Appel, M.; Beck, W.; Phillips, J. R.; Trogler, W. C. *Organometallics* **1990**, *9*, 1296.

Table 2. Comparison of ^{13}C NMR, IR, and Structural Parameters of $L_mM-(\mu\text{-}C_n)-ML_m$ and L_mM-C_nH Complexes

		^{13}C NMR/ppm				bond lengths/Å			
ML_m	C_n	C_α	C_β	C_γ	C_δ	C≡C	C−C	ν(C≡C)/cm^{-1}	ref
$FeCp^*(CO)_2$ (Fp*; **1**)	C_2H	97.0	97.5			1.173(4)			5b
$FeCp(CO)_2$	C_2H	101.4[a]	84.1[a]						7
FeCp(dppe)	C_2H	105.7	68.3					1925	10
FeCp*(dppe)	C_2H	129.5	102.7					1910	11b
$RuCp(PMe_2Ph)_2$	C_2H	108.7	93.3					1925	12b
Ru(dppe)Cl	C_2H	112.0	97.4			1.162(9)		1935	13
$Ru(CO)_2(PEt_3)_2$	C_2H	98.5	95.0			1.199(2)		1944	14
$ReCp^*(NO)(PPh_3)$	C_2H	98.0	116.0					1939	4b
$ScCp^*_2$	C_2H	99.9							15
H	C_2H	71.9	71.9			1.20		1947	16
$FeCp^*(CO)_2$ (Fp*; **2**)	μ-C_2	98.1	98.1			1.202(5)			5b
$RuCp(CO)_2$	μ-C_2	74.7	74.7			1.19(1)			12a
$Re(CO)_5$	μ-C_2	94.4	94.4			1.20(3)		2002[b]	17
$WCp(CO)_3$	μ-C_2	101.1	101.1			1.18(3)			18
$Pt(PMe_3)_2I$	μ-C_2					1.18(5)		2022[b]	3d
$ScCp^*_2$	μ-C_2	179.4	179.4			1.224(7)		1899[b]	15
$ReCp^*(NO)(PPh_3)$[c] $Pd(PEt_3)_2Cl$	μ-C_2	111.7[d]	116.2[d]			1.21(1)			4a
$RuCp(PMe_3)_2$[c] $ZrCp_2Cl$	μ-C_2	178.3[e]	190.4[e]			1.25(2)		1868	19
$FeCp^*(CO)_2$ (Fp*; **3**)	C_4H	106.4	92.8	71.9	53.5	1.207(5)[f] 1.153(6)[g]	1.378(6)	2141	this work
$FeCp(CO)_2$	C_4H	96.8[a]	89.9[a]	70.9[a]	54.4[a]			2109	7
$FeCp(CO)(PPh_3)$	C_4H	109.4	99.1	72.1	54.3			2170	7
FeCp*(dppe)	C_4H	136.6	100.7	75.1	50.5			2099, 1960	11c
$RuCp(PPh_3)_2$	C_4H	116.4	94.4	73.9	128.4			2109	9a
$Ru(CO)_2(PEt_3)_2$	C_4H	101.3	91.7	72.1	54.5	1.194(2)[f] 1.196(3)[g]	1.386(3)	2137	14
$WCp(CO)_3$	C_4H	110.5	71.6	70.1	63.3			2145	9b
$ReCp^*(NO)(PPh_3)$	C_4H	102.1	110.8	72.4	65.2			2115, 2113	4g
H	C_4H	65.3	67.5	67.5	65.3	1.218(2)	1.384(2)		22
$FeCp^*(CO)_2$ (Fp*; **4**)	μ-C_4	79.8[a]	98.5[a]	98.5[a]	79.8[a]	1.197(5)	1.398(7)	2146	this work
$FeCp(CO)_2$	μ-C_4	66.8[a]	101.6[a]	101.6[a]	66.8[a]				7
FeCp*(dppe)	μ-C_4	99.7	110.2	110.2	99.7			1955, 1880	11a,b
$RuCp(PPh_3)_2$	μ-C_4					1.217(4) 1.24(4)	1.370(6) 1.31(4)	1970	9a
$ReCp^*(NO)(PPh_3)$	μ-C_4	95.8	117.5	117.5	95.8	1.202(7)	1.389(5)	1968	4i
$Rh(CO)(PPr^i_3)_2$	μ-C_4	108.1	109.5	109.5	108.1	1.205(5)	1.388(7)		20
$Rh(H)(Cl)(PPr^i_3)_2$	μ-C_4							2010	20
$IrCl(CO)(PPh_3)_2(MeCN)$	μ-C_4	46.9	95.6	95.6	46.9			2183	21b
$Re(CO)_3(Bu^t_2\text{-bipy})$[c]	μ-C_4	117	124	124	117	1.19(2)	1.43(4)	1981	21c
$WCp(CO)_3$	μ-C_4							2145	9a
$FeCp(CO)(PPh_3)$[c] $WCp(CO)_3$	μ-C_4	98.1[h]	117.6[h]	105.1[h]	52.0[h]			21277b	
$M(PR_3)_2X$ (M = Pd, Pt)[c,i]	μ-C_4							1985−2290	3b
$ReCp^*(NO)(PPh_3)$[c] $Pd(PEt_3)_2Cl$	μ-C_4	90.8[j]	116.1[j]	95.0[j]	83.9[j]			1988	4g
$FeCp^*(CO)_2$ (Fp*; **5**)	μ-C_8	110.8[a]	94.8[a]	61.6[a]	51.4[a]			2136, 2088	this work
$ReCp^*(NO)(PPh_3)$	μ-C_8	109.7	113.3	66.6	64.5			2108, 1956	4f
FeCp*(dppe)	μ-C_8	139.5	101.8	62.7	50.6			2109, 1949	11c
$WCp(CO)_3$	μ-C_8	112.4	91.6	63.7	60.9			2190	9b

[a] Tentatively assigned. [b] Determined by Raman spectroscopy. [c] Heterobimetallic complexes. [d] Re−C_α−C_β−Pd. [e] Ru−C_α−C_β−Zr. [f] C_α≡C_β. [g] C_γ≡C_δ. [h] Only C_α can be assigned on the basis of J_{P-C}, and the other signals are arranged according to the increasing order of the δ_C values. [i] $Cl(Bu_3P)_2M-C_4-M'(PBu_3)_2-C_4-M(PBu_3)_2Cl$ (M, M′ = Pt, Pd) and polymers consisting of the $(Bu_3P)_2M-C_4$ repeating unit. [j] Re−C_α−C_β−C_γ−C_δ−Pd.

an increase in the electron density at C_δ. Thus, the effect of the back-donation reaches C_δ, also indicating the contribution of the butatrienylidene structure (Chart 1).

However, the ^{13}C data for polyynyl and polyynediyl complexes cannot always be interpreted in terms of the contribution of cumulenylidene structures, because, in comparison with typical mononuclear vinylidene and cumulenylidene complexes, the α-carbon atoms ($\delta_C(C_\alpha)$) are not deshielded and the separations between the C_α and C_β signals [$\Delta\delta_C = \delta_C(C_\alpha) - \delta_C(C_\beta)$) are quite small (cf. mononuclear vinylidene complexes: $\delta_C(C_\alpha) \sim 300$; $\Delta\delta_C > 150$). We should also take into account the statement by Lichtenberger et al. based on the PES (photoelectron spectroscopy) study of Fp−C≡CR associated with MO calculations.[24] They concluded that the

(18) (a) Chan, M. C.; Tsai, Y. J.; Chen, C. T.; Lin, Y. C.; Tseng, T. W.; Lee, G. H.; Wang, Y. *Organometallics* **1991**, *10*, 378. (b) Yang, Y.-L.; Wang, L. J.-J.; Huang, S.-L.; Chen, M.-C.; Lee, G.-H.; Wang, Y. *Organometallics* **1997**, *16*, 1573.

(19) Lemke, F. R.; Szalda, D. J.; Bullock, R. M. *J. Am. Chem. Soc.* **1991**, *113*, 8466.

(20) (a) Rappert, T.; Nürnberg, O.; Werner, H. *Organometallics* **1993**, *12*, 1359. (b) Gevert, O.; Wolf, J.; Werner, H. *Organometallics* **1996**, *15*, 2806.

(21) (a) Fyfe, H. B.; Mlekuz, M.; Zargarian, D.; Taylor, N. J.; Marder, T. B. *J. Chem. Soc., Chem. Commun.* **1991**, 188. (b) Stang, B. J.; Tykwinski, R. *J. Am. Chem. Soc.* **1992**, *114*, 4411. (c) Yam, V. W.-W.; Lau, V. C.-Y.; Cheung, K.-K. *Organometallics* **1996**, *15*, 1740.

(22) (a) Tanimoto, M.; Kuchitsu, K.; Morino, Y. *Bull. Chem. Soc. Jpn.* **1971**, *44*, 386. (b) Hölzl, F.; Wrackmayer, B. *J. Organomet. Chem.* **1979**, *179*, 394.

(23) Müller, T. E.; Choi, S. W.-K.; Mingos, D. M. P.; Murphy, D.; Williams, D. J.; Yam, V. W.-W. *J. Organomet. Chem.* **1994**, *484*, 209.

Chart 1

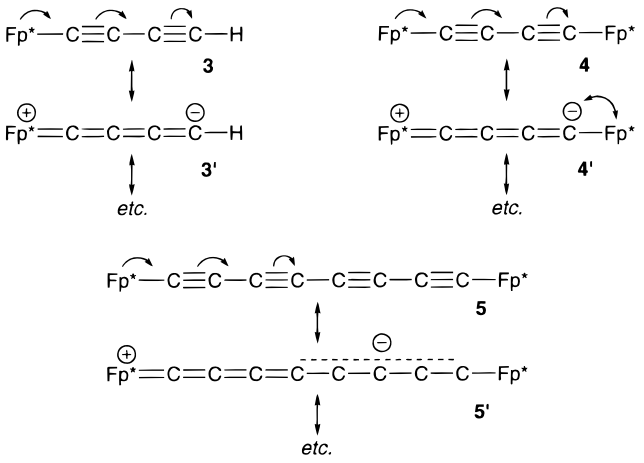

important interaction is the filled/filled one between the occupied metal dπ orbital and the occupied acetylide π bonds rather than the π-back-donation. In the case of the butadiynediyl complex **4**, a tendency opposite to that for **3** and **5** is observed.[25] The charge delocalization in **4** may not be enough to be observed by ^{13}C NMR because of its shorter π-system compared to the C_8 complex (**5**) (Chart 1). In addition, an electrostatic, repulsive interaction between the negative charge developed at C_δ in **4′** and electron donation from the Fp* fragment would also decrease the extent of its contribution. Thus, contribution of the cumulenylidene structure may be more evident in the butadiynediyl complex **3**, having termini with different electron-donating abilities (Fp* and H), and in the octatetraynediyl complex **5**, having a longer π-system, and the order of the carbon signals of **4** is not similar to that of **3** and **5**.

The electronic effect induced by the $(C\equiv C)_n-X$ fragments can be estimated by the ν(CO) values. The averaged values of the two vibrations, symmetric and antisymmetric, of the $Fe(CO)_2$ moiety are in the following order, which corresponds to the electron-accepting ability of the fragments shown in parentheses: 2005 (**5**; C_8-Fp^*) ≈ 2002 (**3**; C_4H) > 1995 (**1**; C_2H) ≈ 1994 (**4**; C_4-Fp^*) ≫ 1974 cm^{-1} (**2**; C_2-Fp^*). This order, which is also supported by the structural study (see below), indicates that, as the carbon chain becomes longer, the electron-accepting ability of the $(C\equiv C)_n-X$ fragment increases. In particular, the competitive back-donation from the two metal centers in the polyynediyl−dimetal complexes (Chart 1) becomes less evident in complexes linked by a longer carbon bridge, in accordance with the above discussion on the ^{13}C NMR data. However, an observation contradictory to the present result was reported by Lichtenberger et al., who arrived at the conclusion that the C_4H ligand is the better π-donor toward the Fp fragment and both have the same σ-donor capability.[24] Although we also have to take into account the considerably small magnitude of the differences in the IR and structural parameters (~10 cm^{-1}, <0.03 Å), the inconsistency may come from the features of the evaluation methods. The ν(CO) values and the structural parameters reflect the net electronic effect of the ligands, whereas the evaluation by Lichtenberger is based mainly on the metal band splitting between the π-type orbitals of $Fp-(C\equiv C)_n-H$. In addition, introduction of the more electron-donating Fp* group should make the back-donation more effective.

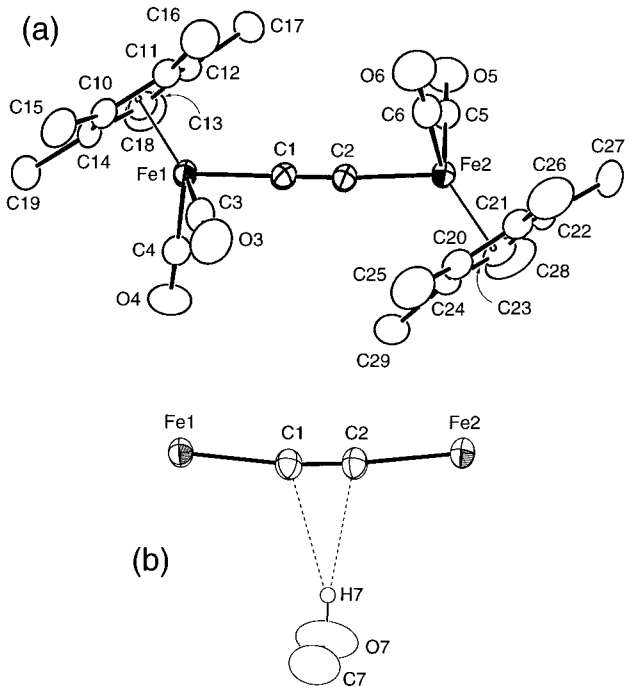

Figure 1. Molecular structure of **2**·MeOH drawn at the 30% probability level: (a) the Fp*−C≡C−Fp* part; (b) interaction with MeOH.

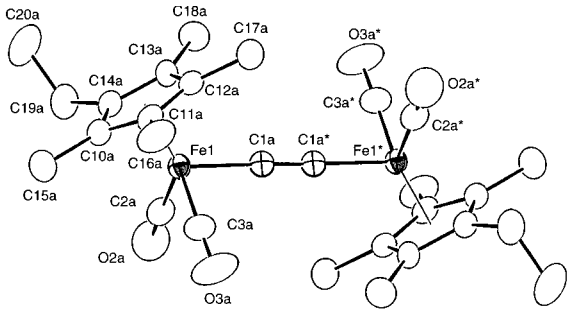

Figure 2. Molecular structure of **2**$^{\#}$ (molecule 1) drawn at the 30% probability level.

Molecular Structure of Fp*−(C≡C)$_n$−Fp* (n = 1, 2) and Fp*−(C≡C)$_n$−H (n = 1, 2). The molecular structures of the ethynediyl (**2** and **2**$^{\#}$), butadiynyl (**3**), and butadiynediyl complexes (**4**) have been determined by X-ray crystallography. ORTEP views are reproduced in Figures 1 −4, and pertinent structural parameters are summarized in Chart 2 together with those of the ethynyl complex (**1**) reported previously.[5b]

The polyynyl and polyynediyl complexes have a linear rodlike linkage. The C≡C and C−C distances are in the narrow ranges of 1.173−1.211 and 1.378−1.396 Å, respectively, which are comparable to those in ethyne (C≡C:,1.20 Å),[16] butadiyne (C≡C, 1.218(2) Å; C−C, 1.384(2) Å),[22] and the previously reported M−(C≡C)$_n$-H- and M−(C≡C)$_n$-M-type complexes as compared in

(24) (a) Lichtenberger, D. L.; Renshaw, S. K.; Wong, A.; Tagge, C. D. *Organometallics* **1993**, *12*, 3522. See also: (b) Lichtenberger, D. L.; Renshaw, S. K.; Bullock, R. M. *J. Am. Chem. Soc.* **1993**, *115*, 3276.

(25) The ^{13}C NMR data for the ethynyliron complexes (η^5-C_5R_5)Fe(L)$_2$(C≡CH) also cannot always be interpreted in terms of back-donation alone. Replacement of the supporting ligands (η^5-C_5R_5 and L) by a more electron-donating one (Cp vs Cp*; (CO)$_2$ vs dppe) does not always cause the deshielding of the α-carbon signal (Table 2) or a monotonous increase in separation of the two signals ($\delta_C(C_\alpha) - \delta_C(C_\beta)$: −0.5 (Fp*; **1**); 17.0 (FeCp(CO)$_2$); 37.4 (FeCp(dppe)); 26.8 (FeCp*(dppe))).

Chart 2

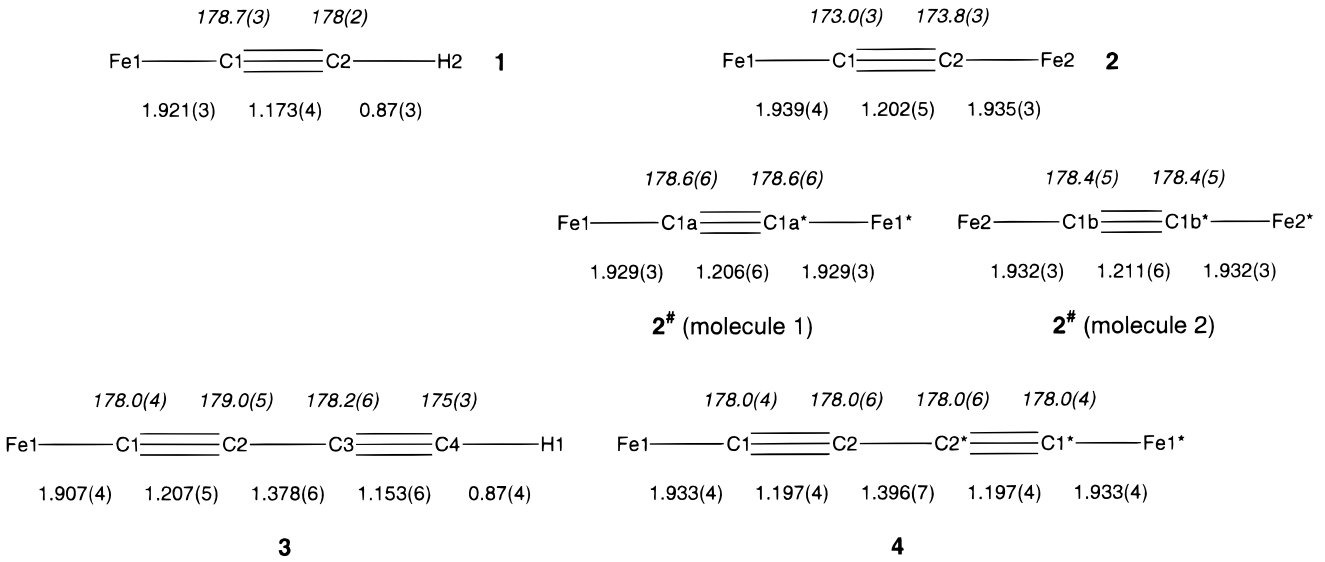

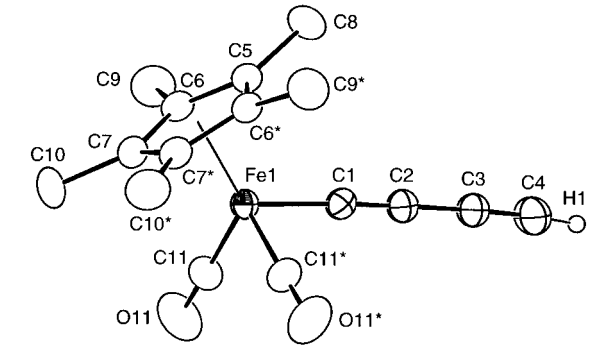

Figure 3. Molecular structure of **3** drawn at the 30% probability level.

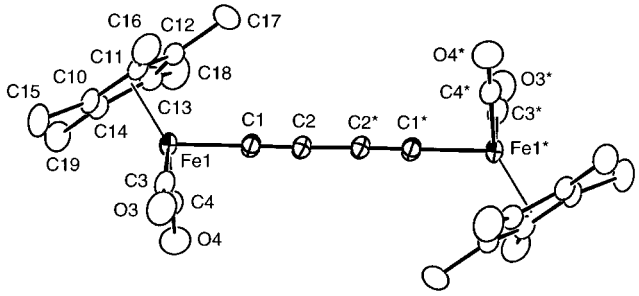

Figure 4. Molecular structure of **4** drawn at the 30% probability level.

Table 2. The Fe···Fe distances are 5.052(1) (**2**), 5.063(1) (**2**$^{\#}$; molecule 1), 5.075(1) (**2**$^{\#}$; molecule 2), and 7.653(1) Å (**4**).

It is notable that the Fe−C≡C−Fe linkage in **2** (~173°) is slightly deviated from a linear structure due to a hydrogen-bonding interaction with the acidic methanol hydrogen atom, as can be seen in Figure 1b, and no such structural distortion is observed for the Fp$^{\#}$ derivative (**2**$^{\#}$; Figure 2). A unit cell of **2**$^{\#}$ contains two crystallographically independent molecules with essentially the same structure. (An ORTEP view of molecule 2 is reproduced in the Supporting Information.) The Fe−C≡C−Fe linkage of **2** is bent away from the MeOH part, and the distances between the methanol oxygen atom (O7) and the C≡C atoms (3.213(6) (C1) and 3.193(6) Å (C2)) fall in the range of hydrogen-bonding interactions. The methanol hydrogen atom (H7) refined isotropically is directed toward the C≡C moiety with separations of 2.45(5) Å (to C1) and 2.41(5) Å (to C2). Such hydrogen-bonding interactions have been often found for acetylide complexes bearing an electron-donating metal fragment. For example, it was reported that even chloroform could form a 1:2 adduct with the highly basic gold complex $(R_3P)Au-C\equiv C-Au(PR_3)$, through a hydrogen-bonding interaction, as reported by Mingos et al.[23]

When the structures of **1** and **3** are inspected in detail, the Fe1−C1 distance in **3** is shorter than that in **1** (by 0.014 Å) and, in contrast, the C1−C2 distance in **3** is longer than that in **1** (by 0.034 Å). This structural deformation may also be attributed to the contribution of the butatrienylidene structure to **3** (Chart 1), and the C_4H ligand turns out to be more electron-accepting than the C_2H ligand. As for the ≡C−C≡ distance, the C2−C3 distance in **3** is shorter than the C2−C2* distance in **4** (by 0.018 Å) and is comparable to the ≡C−C≡ distance in HC≡C−C≡CH (1.384(2) Å). The competitive back-donation from the two metal centers in **4** may cancel out the contribution of the cumulenylidene structure as discussed above, and therefore, the Fe−C distance in the symmetrical complexes, in particular, the butadiynediyl complexes (**4**), is longer than that in the unsymmetrical complexes **1** and **3**. In **3** the effect does not appear to reach the C3≡C4 moiety, as judged by its unaffected bond length, but ^{13}C NMR data discussed above clearly indicate a substantial contribution of such a structure. These structural features are in accord with the discussion on the electron-accepting ability of the $(C\equiv C)_n-X$ fragments based on the δ_C and $\nu(C\equiv O)$ values (see above).

Experimental Section

General Considerations. All manipulations were carried out under an inert atmosphere by using standard Schlenk tube techniques. Ether, hexanes (Na−K alloy), and CH_2Cl_2 (P_2O_5) were treated with appropriate drying agents, distilled, and stored under argon. Fp*−Cl,[26] Fp*−I,[26] Fp$^{\#}$−Cl,[26] Fp$^{\#}$−I,[26] and

(26) Akita, M.; Terada, M.; Tanaka, M.; Moro-oka, Y. *J. Organomet. Chem.* **1996**, *510*, 255.

Table 3. Crystallographic Data

	2·MeOH	**2**#	**3**	**4**
formula	$C_{27}H_{34}O_5Fe_2$	$C_{28}H_{34}O_4Fe_2$	$C_{16}H_{16}O_2Fe$	$C_{28}H_{30}O_4Fe_2$
fw	550.3	546.3	296.2	542.2
cryst syst	monoclinic	monoclinic	monoclinic	monoclinic
space group	$P2_1/c$	$P2_1/n$	$P2_1/m$	$P2_1/n$
a/Å	11.652(3)	18.862(4)	7.241(3)	8.790(2)
b/Å	13.632(5)	8.024(7)	11.820(5)	11.894(2)
c/Å	17.253(4)	19.323(5)	8.737(4)	12.429(2)
β/deg	95.35(2)	109.75(2)	99.56(3)	99.50(1)
V/ Å^3	2728(2)	2752(2)	737.4(5)	1281.5(3)
Z	4	4	2	2
d_{calcd}/g cm^{-3}	1.34	1.32	1.33	1.41
μ/cm^{-1}	10.9	10.8	10.2	11.6
2θ/deg	5−50	5−55	5−50	5−50
no. of data collected	5284	6968	2413	3282
no. of data with $I > 3\sigma(I)$	3600	4243	1391	1785
no. of variables	311	443	131	214
R	0.038	0.046	0.045	0.040
R_w	0.042	0.031	0.031	0.028

bis(trimethylsilyl)butadiyne[27] were prepared according to the published methods. Other chemicals were purchased and used as received. Chromatography was performed on alumina (aluminum oxide, activity II−IV (Merck Art. No. 1097)). ^{1}H and ^{13}C NMR spectra were recorded on JEOL EX-400 (^{1}H, 400 MHz; ^{13}C, 100 MHz) and Bruker AC-200 spectrometers (^{1}H, 200 MHz). Solvents for NMR measurements containing 0.5% TMS were dried over molecular sieves, degassed, distilled under reduced pressure, and stored under Ar. IR spectra were obtained on a JASCO FT/IR 5300 spectrometer.

Preparation of Fp*−C≡C−Fp* (2) and Fp#−C≡C−Fp# (2#). Complex **2** was prepared by a modified method.[5c] To a THF solution (16 mL) of [Fp*$_2$(μ-C≡C-H)]BF$_4$[5b] (1.59 g, 2.63 mmol) was added NEt_3 (0.48 mL, 3.42 mmol) at room temperature. After the mixture was stirred for 1 h, the volatiles were removed under reduced pressure. Products were extracted with ether and passed through an alumina plug to remove salts. Addition of hexanes and cooling to −20 °C gave **2** (0.94 g, 1.83 mmol, 70% yield) as brick red crystals.

The Fp# derivative **2**# was prepared in 75% yield in a manner similar to the synthesis of **2**. **2**#: ^{1}H NMR ($CDCl_3$) δ 1.01 (6H, t, J = 7.7 Hz, CH_2CH_3), 1.81 (24H, s, C_5Me_4), 2.26 (4H, q, J = 7.7 Hz, CH_2CH_3); ^{13}C NMR ($CDCl_3$) δ 9.7, 9.9 (q × 2, J = 130 Hz, C_5Me_4Et), 14.5 (q, J = 130 Hz, $C_5Me_4CH_2CH_3$), 18.3 (t, J = 129 Hz, $C_5Me_4CH_2CH_3$), 95.5, 96.8 (s × 2, C_5Me_4Et), 97.6 (s, C≡C), 100.0 (s, C_5Me_4Et); IR (KBr) 1992, 1942 cm^{-1}. Anal. Calcd for $C_{28}H_{34}O_4Fe_2$: C, 61.59; H, 6.23. Found: C, 61.68; H, 6.02.

Preparation of Fp*−C≡CC≡CH (3). To a THF solution (10 mL) of Me_3Si−C≡CC≡C$SiMe_3$ (1.46 g, 7.512 mmol) was added an ethereal solution of MeLi (1.4 M, 4.6 mL, 6.4 mmol), and the resulting mixture was stirred for 3.5 h at ambient temperature. The resulting solution was added to a THF solution (12 mL) of Fp*−I (2.00 g, 5.35 mmol) cooled to −78 °C. After the mixture was stirred for 10 min at the same temperature, the cooling bath was removed and stirring was continued for 4.5 h at ambient temperature. Then completion of the reaction was checked by TLC, and 1 mL of MeOH was added to destroy the excess MeLi. The volatiles were removed under reduced pressure, and products were extracted with ether and passed through an alumina plug. Addition of hexanes gave Fp*−C≡CC≡C$SiMe_3$ as brown-yellow precipitates, which were collected (1.32 g, 3.59 mmol). Cooling the supernatant solution gave additional product (398 mg, 1.08 mmol). Total yield: 87%. ^{1}H NMR ($CDCl_3$): δ 1.85 (15H, s, Cp*), 0.14 (9H, s, $SiMe_3$). IR (KBr): 2178, 2125, 2030, 2010, 1964 cm^{-1}. IR (CH_2Cl_2): 2170, 2119, 2033, 2015, 1977 cm^{-1}. Anal. Calcd for $C_{19}H_{24}O_2FeSi$: C, 61.96; H, 6.57. Found: C, 61.70; H, 6.50.

To a THF solution (20 mL) of Fp*−C≡CC≡C−$SiMe_3$ (946 mg, 2.57 mmol) was added Bu_4NF (1 M THF solution, 0.3 mL, 0.3 mmol), and the resulting mixture was stirred for 1 h at room temperature. After the conversion to **3** was confirmed by TLC, the volatiles were removed under reduced pressure. Products were extracted with CH_2Cl_2 and passed through an alumina plug. Addition of hexanes to the filtrate gave **3** as a yellow powder (702 mg, 2.37 mmol, 92% yield). Complex **3** could be purified by crystallization from CH_2Cl_2−hexanes. Anal. Calcd for $C_{16}H_{16}O_2Fe$: C, 64.89; H, 5.44. Found: C, 64.58; H, 5.31.

Preparation of Fp*−C≡CC≡C−Fp* (4) (Method I). To a THF solution (20 mL) of **3** (500 mg, 1.69 mmol) cooled to −78 °C was added *s*-BuLi (1.08 M, cyclohexane solution, 1.85 mL, 2.0 mmol), and the mixture was further stirred for 10 min at the same temperature. Then Fp*−Cl (613 mg, 2.34 mmol) dissolved in THF (4 mL) was added to the resulting solution dropwise, and the mixture was stirred for 10 min at −78 °C and then for 24 h at room temperature. After the conversion of **3** was checked by TLC, MeOH (1 mL) was added and the volatiles were removed under reduced pressure. Products were extracted with CH_2Cl_2 and were subjected to column chromatography (CH_2Cl_2−hexanes, (1:3)−(3:1)). The product **4** was isolated from the orange band as orange powders (231 mg, 0.426 mmol, 25% yield). Single crystals of **4** were obtained by crystallization from toluene−MeOH. Anal. Calcd for $C_{28}H_{30}O_4Fe_2$: C, 62.02; H, 5.58. Found: C, 61.85; H, 5.45.

Preparation of Fp*−C≡CC≡C−Fp* (4) (Method II). CuI (200 mg, 1.05 mmol) was added to NEt_3 (20 mL, degassed under reduced pressure), and the resulting suspension was stirred for 10 min. The resulting mixture was added to a THF solution (40 mL) of **3** (1.00 g, 3,39 mmol) in one portion. After the mixture was stirred for 30 min at room temperature, Fp*−Cl (1.05 g, 3.73 mmol) dissolved in THF (12 mL) was added, and the resulting mixture was further stirred for 7 h (orange precipitates appeared). After evaporation of the solvents the products were extracted with CH_2Cl_2 and passed through an alumina plug. Removal of the solvent under reduced pressure gave orange precipitates, which were washed with ether. **4**: 1.56 g, 2.89 mmol, 85% yield.

Preparation of Fp*−C≡CC≡CC≡CC≡C−Fp* (5). To a degassed suspension of CuCl (100 mg, 1.01 mmol) in acetone (12 mL) was added TMEDA (0.2 mL, 1.3 mmol), and the resulting mixture was stirred vigorously for 30 min. The supernatant blue-green solution was used as CuCl·TMEDA. In a flask equipped with a rubber septum, a gas inlet and outlet, and a thermometer, the butadiynyl complex **4** (504 mg, 1.70 mmol) was weighed, and acetone (55 mL) was added. Oxygen gas was passed through the resulting solution from the gas inlet. Then, the CuCl·TMEDA solution was added portionwise (1 mL each) through the rubber septum via a syringe, while the vigorous stirring and O_2 bubbling were maintained (∼30 min). The addition rate was adjusted so that the temperature did not exceed 30 °C. The stirring and O_2 bubbling were continued for 3 h. Then, the volatiles were removed under reduced pressure and the residue was extracted with CH_2Cl_2, which was passed through a short alumina plug. The filtrate was removed under reduced pressure. The resulting orange precipitates were washed with CH_2Cl_2, Et_2O, and hexanes successively and dried under reduced pressure. **5**: yellow-brown powder, 377 mg, 0.639 mmol, 75% yield. Anal. Calcd for $C_{32}H_{30}O_4Fe_2$: C, 65.11; H, 5.12. Found: C, 63.76; H, 5.10. An analytically pure sample has not been obtained despite several attempts.

Experimental Procedure for X-ray Crystallography. Single crystals of **2**·MeOH, **2**#, **3**, and **4** were obtained by recrystallization from toluene−MeOH, Et_2O−hexanes, CH_2Cl_2−hexanes, and toluene−MeOH, respectively. Suitable single crystals were mounted on glass fibers, and diffraction measurements were made on Rigaku AFC-5R (**2**·MeOH, **3**, **4**) and AFC-7R (**2**#) automated four-circle diffractometers by using graphite-monochromated Mo Kα radiation (λ = 0.710 59

(27) (a) Jones, G. E.; Kendrick, D. A.; Holmes, A. B. *Org. Synth.* **1987**, *65*, 52. (b) Holmes, A. B.; Sporikou, C. N. *Org. Synth.* **1987**, *65*, 61.

Å). The unit cells were determined and refined by a least-squares method using 20 independent reflections ($2\theta \approx 20°$). Data were collected with an $\omega-2\theta$ scan technique. If $\sigma(F)/F$ was more than 0.1, a scan was repeated up to three times and the results were added to the first scan. Three standard reflections were monitored every 150 measurements. The data processing was performed on a Micro Vax II computer (data collection) and IRIS Indigo and Indy computers (structure analysis) by using the teXsan structure solving program system obtained from the Rigaku Corp., Tokyo, Japan. Neutral scattering factors were obtained from the standard source.[28] In the reduction of data, Lorentz and polarization corrections and an empirical absorption correction (Ψ scan) were made. Crystallographic data and the results of refinements are summarized in Table 3.

The structures were solved by a combination of direct methods (SAPI91 and MITHRIL87) and Fourier synthesis (DIRDIF). All the non-hydrogen atoms were refined with anisotropic thermal parameters. The MeO*H* atom (H7) in **2**·MeOH and all the hydrogen atoms in **2**$^{\#}$, **3**, and **4** were refined isotropically, and the Cp* and CH_3O hydrogen atoms in **2**·MeOH were fixed at calculated positions (C−H = 0.95 Å) and were not refined.

Acknowledgment. We are grateful to the Ministry of Education, Science, Sports and Culture of the Japanese Government for financial support of this research.

Supporting Information Available: Figures giving the atomic numbering schemes for the hydrogen atoms of **2**, **2**$^{\#}$, **3,** and **4** and tables of positional parameters and B_{eq} values, anisotropic thermal parameters, and bond lengths and angles for these compounds (16 pages). Ordering information is given on any current masthead page.

OM970538M

(28) Int*ernational Tables for Crystallography*; Kynoch Press: Birmingham, U.K., 1975; Vol. 4.